01 Jan 2010

An Adaptive Control Strategy for DSTATCOM Applications in an Electric Ship Power System

Pinaki Mitra

Ganesh K. Venayagamoorthy
Missouri University of Science and Technology

An Adaptive Control Strategy for DSTATCOM Applications in an Electric Ship Power System

Pinaki Mitra, *Student Member, IEEE*, and Ganesh Kumar Venayagamoorthy, *Senior Member, IEEE*

Abstract—**Distribution static compensator (DSTATCOM) is a shunt compensation device that is generally used to solve power quality problems in distribution systems. In an all-electric ship power system, power quality issues arise due to high-energy demand loads such as pulse loads. This paper presents the application of a DSTATCOM to improve the power quality in a ship power system during and after pulse loads. The control strategy of the DSTATCOM plays an important role in maintaining the voltage at the point of common coupling. A novel adaptive control strategy for the DSTATCOM based on artificial immune system (AIS) is presented in this paper. The optimal parameters of the controller are first obtained by using the particle swarm optimization algorithm. This provides a sort of innate immunity (robustness) to common system disturbances. For unknown and random system disturbances, the controller parameters are modified online, thus providing adaptive immunity to the control system. The performance of the DSTATCOM and the AIS-based adaptive control strategy is first investigated in MATLAB-/Simulink-based simulation platform. It is verified through a real-time ship power system implementation on a real-time digital simulator and the control algorithm on a digital signal processor.**

Index Terms—**Adaptive control, adaptive immunity, artificial immune system (AIS), digital signal processor (DSP), distribution static compensator (DSTATCOM), electric ship power system, innate immunity, real-time digital simulator (RTDS).**

I. INTRODUCTION

THE POWER system of an all-electric navy ship has an integrated network, where the propulsion load, the distribution loads, sensor and other emergency loads, and pulse loads (rail guns, aircraft launchers, etc.) all are part of the same electrical network. Among the loads, the effects of pulse loads are most detrimental for the power quality of ship power distribution system, as they require a very high amount of energy for a very short period of time [1], [2]. In order to improve the survivability of a navy ship in battle conditions, a distribution static compensator (DSTATCOM) can be used to reduce the impact of pulse loads on the bus voltage, and thus, keep it at desired level. DSTATCOM is a voltage-source inverter (VSI) based shunt device [3], which is generally used in distribution system to improve power quality. The main advantage of DSTATCOM is that the current injection into the distribution

bus can be regulated very efficiently by the sophisticated power-electronics-based control present in it. Another advantage is that it has multifarious applications, e.g., it can be used for canceling the effect of poor load power factor, for suppressing the effect of harmonic content in load currents, for regulating the voltage of distribution bus against sag/swell, etc., for compensating the reactive power requirement of the load, etc. [4]. In this paper, the application of DSTATCOM to regulate voltage at the point of common coupling (PCC) is presented.

The internal controls of a DSTATCOM play a very important role in the effectiveness of the DSTATCOM in maintaining the PCC voltage during pulse loads. Most of the research in DSTATCOM has focused on topology and its applications. For example, different control strategies based on the respective multilevel inverter topologies of shunt compensators are discussed in [3] and also in [5]–[7]. A robust controller, sliding-mode control strategy, is adopted in [8] and [9]. But, these control strategies are not adaptive to changes in the system dynamics, and hence, the performance may not be satisfactory for unknown and random system disturbances. These types of disturbances are inevitable in naval shipboard systems, especially in battle conditions. Different ranges of rail guns and launchers may be used leading to a wide variation of pulse power disturbances. Adaptive control of a DSTATCOM becomes essential for survivability. Conventional controllers for DSTATCOMs are mainly based on proportional–integral (PI) controllers. The tuning of PI controllers is a complex task for a nonlinear system with lot of switching devices. In order to overcome these problems, computational intelligence (CI) techniques can be used. Application of CI techniques in designing adaptive controller for DSTATCOM is not yet explored much by the researchers. The study in [10] and [11] is based on neural networks (NNs). The PI controllers are replaced by a NN trained with the backpropagation algorithm in [10]. But, the training is carried out offline, and hence, the artificial neural network (ANN) based controller is not adaptive. An NN-based reference current generator is used in [11], which is a partially adaptive control strategy. Here, though the reference generator adapts its NN weights online, but the dc voltage regulation is handled by conventional PI controllers.

In this paper, a new adaptive control strategy for a DSTATCOM based on artificial immune system (AIS) is presented. Most of the CI techniques are offline, and require prior knowledge of the system behavior. But AIS, which is inspired by theoretical immunology and observed immune functions, principles, and models, has the potential for online adaptive system identification and control [12]. Abnormal changes in the system response are identified and acted upon without having any prior knowledge [13]. The AIS-based DSTATCOM controller

Fig. 1.　Schematic diagram of DSTATCOM.

Fig. 2.　Control structure for the DSTATCOM for MATLAB implementation.
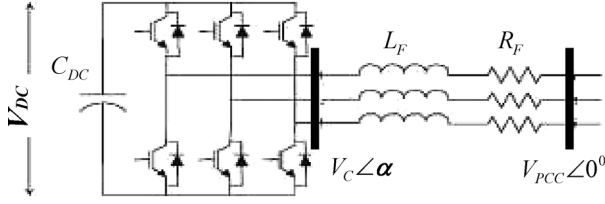
exhibits innate and adaptive immune system behaviors. Innate response is for common disturbances, and requires controller parameters to be optimal. In this paper, the innate controller parameters are determined using the particle swarm optimization (PSO) algorithm. The adaptive response is for new and unusual disturbances, and requires the controller parameters to be adaptive. The AIS strategy is applied in this paper for adaptation of these parameters.

The adaptive control strategy for a DSTATCOM in a shipboard power system is first investigated in the MATLAB-/Simulink-based simulation environment [14]. Based on the satisfactory performance, it is then implemented on a platform consisting of a real-time digital simulator (RTDS) and a digital signal processor (DSP). The advantage of RTDS is that it can represent the dynamics of a system close to a practical system. The fast-acting power electronic switching devices are also simulated in such a way that it can be interfaced with a practical hardware system any time. The tuning of the controller parameters using PSO to exhibit innate response as well as the AIS-based control strategy to exhibit adaptive response are implemented on a DSP interfaced to the RTDS.

II. DSTATCOM AND ITS CONTROL STRUCTURE

The simplest structure of a DSTATCOM is shown in Fig. 1. The principle of operation of DSTATCOM is based on the fact that the real and reactive powers can be varied by the voltage magnitude (V_C) of the inverter, and the angle difference between the bus and the inverter output (α). The active and reactive power are expressed as follows:

$$P = \frac{V_{\mathrm{PCC}} V_C \sin \alpha}{X} \tag{1}$$

$$Q = \frac{V_{\mathrm{PCC}}(V_{\mathrm{PCC}} - V_C \cos \alpha)}{X} \tag{2}$$

where

P　　　active power;
Q　　　reactive power;
V_C　　inverter voltage;
V_{PCC}　voltage at the PCC;
α　　　angle of V_{PCC} with respect to V_C;
X　　　reactance of the branch and the transformer.

In steady-state operation, the angle α is very close to zero. Now, if $V_{\mathrm{PCC}} < V_C$, reactive power flows from the DSTATCOM to the bus. So, by controlling the inverter voltage magnitude V_C, the reactive power flow from the DSTATCOM can be regulated. This can be done in several ways. In this paper, two different types of control strategies for DSTATCOM are considered.
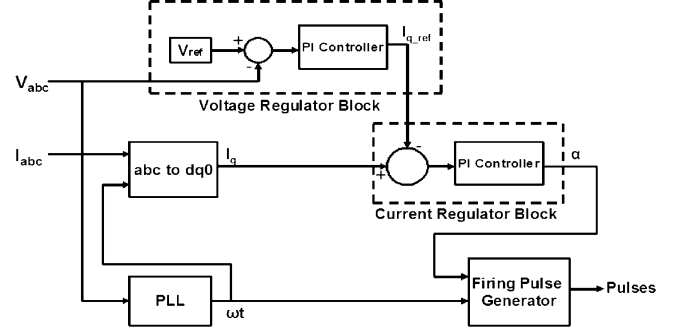
The first type of control strategy is employed for the MATLAB-based simulation. Here, a gate turn-off thyristor (GTO)-based square-wave voltage-source converter (VSC) is used to generate the alternating voltage from the dc bus. In this type of inverters, the fundamental component of the inverter output voltage is proportional to the dc bus voltage. So, the control objective is to regulate V_{dc} as per requirement. Also, the phase angle should be maintained so that the ac-generated voltage is in phase with the bus voltage. The schematic diagram of the control circuit is shown in Fig. 2.

Here, the PLL synchronizes the GTO pulses to the system voltage and generates a reference angle. This reference angle is used to calculate positive sequence component of the DSTATCOM current using a–b–c to d–q–0 transformation. The voltage regulator block calculates the difference between reference voltage and measured bus voltage, and the output is passed through a PI controller to generate the reactive current reference I_{q_ref}. This I_{q_ref} is then passed through a current regulator block to generate the angle α. This current regulator block also consists of a PI controller to keep the angle α close to zero.

The "firing pulse generator" block generates square pulses for the inverter from the output of the PLL and the current regulator block. If due to the application of a pulse load the bus voltage reduces to some extent, the voltage regulator changes the I_{q_ref}, and as a result, the current regulator increases the angle α so that more active power flows from bus to the DSTATCOM and energizes the capacitor. So, the dc voltage increases, and consequently, the ac output of the inverter also increases, and the necessary reactive power flows from DSTATCOM to the bus.

The second type of control strategy consists of insulated-gate bipolar transistor (IGBT) based inverter, and is employed for the real-time implementation. It is represented in Fig. 3.

Here, the PLL generates a reference angle. This reference angle is used to calculate d–q component of the DSTATCOM current using a–b–c to d–q–0 transformation. Also this angle is used to calculate the a–b–c voltage from its d and q components, and to generate a triangular wave for the sine-triangle modulator to produce required firing pulses. The controller uses a two-layer decoupled control scheme to keep the bus voltage and the dc capacitor voltage at constant level [15]. The PI controllers of the outer layer [PI(1) and PI(2)] generate the reference currents I_{d_ref} and I_{q_ref} for the inner loop. The other two PI controllers [PI(3) and PI(4)] just keeps track of the reference.
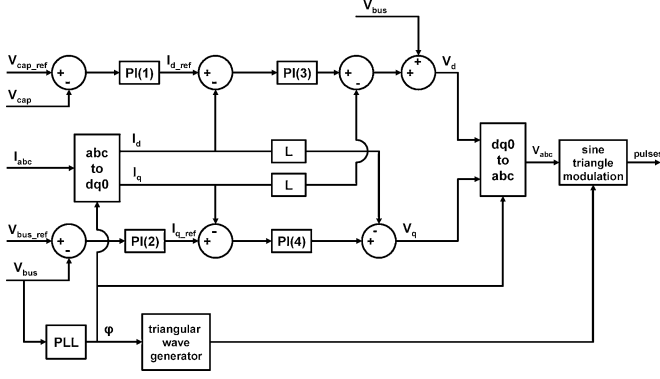
Fig. 3.   DSTATCOM control structure for an RTDS implementation.

III. PSO-Based Tuning of DSTATCOM Controller

For both the control strategies, the optimal values of the PI controller parameters are first tuned by PSO algorithm. PSO is a population-based search algorithm modeled after the motion of flock of birds and school of fish [16]. A swarm is considered to be a collection of particles, where each particle represents a potential solution to a given problem. The particles "fly" over the search space to find the optimal solution [16]. The velocity and position of the ith particle of d dimension is updated by the following equations:

$$v_{id}(k+1) = wv_{id}(k) + c_1 \, \text{rand}_1 \, (x_{p\text{best}\_id}(k) - x_{id}(k))$$
$$+ c_2 \, \text{rand}_2 \, (x_{g\text{best}\_id}(k) - x_{id}(k)) \quad (3)$$

$$x_{id}(k+1) = x_{id}(k) + v_{id}(k+1) \quad (4)$$

where $x_{id}(k)$ and $x_{id}(k+1)$ are the positions, $v_{id}(k)$ and $v_{id}(k+1)$ are the velocities of the ith particle with d dimensions at instants k and $(k+1)$, respectively, $x_{p\,\text{best}\_id}(k)$ and $x_{g\,\text{best}\_id}(k)$ are the previous best and global best positions of the particles at the kth instant, w is the inertia weight, and c_1 and c_2 are the cognitive and social acceleration constants, respectively.

Now, for the first type of control strategy (simulated in MATLAB), in order to find out the optimum DSTATCOM controller parameters using the PSO algorithm, the four parameters (Kpv = proportional gain of the voltage regulator block, Kiv = integral gain of the voltage regulator block, Kpc = proportional gain of the current regulator block, and Kic = integral gain of the current regulator block) are considered to be the four dimensions of each particle in the swarm. Here, bus voltage regulation is one of the main objectives of the DSTATCOM. Hence, the cost function is considered in such a way that it minimizes the area swept out by the bus voltage curve above and below the steady-state value of the bus voltage during and after the pulse load application. The mathematical expression for the cost function is given by

$$J = \sum_{k=1}^{T/\Delta t} \frac{1}{2} (|\Delta v(k)| + |\Delta v(k+1)|) \Delta t \quad (5)$$

where

T total time of simulation after the application of the pulse load;

Δt sampling interval;

k sampling instant;

$\Delta v(k)$ bus voltage deviation at the kth sampling instant.

To have a fast PSO search performance, the values of w, c_1, and c_2 are kept fixed at 0.8, 2.0, and 2.0, respectively, and the number of particles taken is 25 [16]. The optimum PI controller parameters found by PSO are $Kpv = 20.0$, $Kiv = 1462.5$, $Kpc = 20.2$, and $Kic = 35.1$.

For the second type of control strategy, which is implemented on the RTDS, a real-time PSO-based tuning of controller parameters is implemented. In this type of control, the performance of a DSTATCOM strongly depends on the PI controllers of the external loop that generate the current references. Hence, in this paper, these two PI controllers, [PI(1) and PI(2)] in Fig. 3, are tuned using PSO. The PSO algorithm is implemented on an Innovative Integration M67 card, which is based on the Texas Instruments TMS3206701 DSP. The M67 operates at 160 MHz, and is equipped with two A/D conversion and digital-to-analog (D/A) conversion modules. The rest of the system is built in real-time simulator computer aided design (RSCAD) software suite, which is the software developed by RTDS for use with the real-time digital simulator. The analog signal provided to the M67 is the ac bus voltage deviation ($\Delta v(k)$), which comes from the RTDS. This is converted to digital signal through the A/D block of the DSP, and is used to calculate the fitness value of the controller parameters. The cost function is considered to be the same as (5). The four parameters [K_{p1} = proportional gain of PI(1), K_{i1} = integral gain of PI(1), K_{p2} = proportional gain of PI(2), and K_{i2} = integral gain of PI(2)] are the dimensions of each particle of the swarm. The particle positions are initiated randomly inside the DSP and are sent to the RTDS as analog voltage signals within the range of -10 to $+10$ V. These voltages are scaled proportionately inside the RTDS and used as the PI controller parameters for each iteration. The calculation of $p$best and $g$best, and the update of position and velocity are all performed by the DSP. The laboratory hardware setup for this study is shown in Fig. 4. The optimum PI controller parameters found by PSO are $K_{p1} = 30.0$, $K_{i1} = 50.02$, $K_{p2} = 124.7$, and $K_{i2} = 2.08$.

IV. Biological Immune System and Adaptive Controller Design

The natural immune system of a human body is basically the interaction of various cells. Among these, T and B cells play the most vital roles. B cells secrete antibodies, whereas, T cells are made of three types of cells: 1) helper T cells; 2) suppressor T cells; 3) killer T cells. Within the immune system, there is a feedback mechanism. When a nonself cell (antigen) is identified in a human body by the antigen presenting cell (APC), it activates helper T cells. These helper T cells then stimulate the B cells, the killer T cells, and the suppressor T cells. Activation of B cell is the most important feedback mechanism of the immune system, and is basically responsible for elimination of antigens. Again, when the number of antigens is reduced, the suppressor T cells inhibit the activities of all other cells. As a result of this inhibitive feedback mechanism, the action of immune system is tranquilized [12].

The approach to adapt parameters of the two PI controllers, which are already found by PSO for innate immunity, is
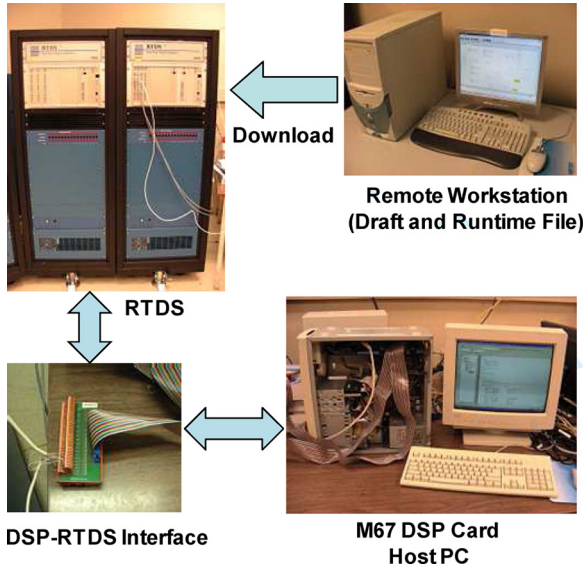
Fig. 4.   Laboratory hardware setup including RTDS and DSP.

Fig. 5.   AIS-based adaptive control strategy of a DSTATCOM.

described next. The discussion is presented with reference to the second control strategy that is implemented on the RTDS. A similar approach is also followed for the MATLAB-based test system. In order to avoid repetition, it is not discussed separately.

The amount of foreign material (antigen) at kth generation is defined here as the deviation in the PCC bus voltage $\Delta V_b(k)$, and also as the deviation of the capacitor voltage $\Delta V_{\rm CAP}(k)$. The first PI controller's [PI(1)] objective is to maintain the capacitor voltage constant, i.e., $\Delta V_{\rm CAP}(k)$ should be zero. Similarly, the other PI controller [PI(2)] should keep $\Delta V_b(k)$ equal to zero. In terms of AIS, the aforesaid functions of the PI controllers can be made adaptive by considering the actions of the helper and suppressor T cells. The mathematical representation shown here is only for the antigen $\Delta V_b(k)$. The same analysis holds for the antigen $\Delta V_{\rm CAP}(k)$.

The output from the helper T cells stimulated by the antigen $\Delta V_b(k)$ is given by

$$\mathrm{TH}(k) = m\Delta V_b(k) \tag{6}$$

where "m" is the stimulation factor whose sign is positive. The suppressor T cells inhibit the other cell activities, and its effect can be represented by

$$\mathrm{TS}(k) = m'f\left(\frac{\Delta V_b(k)}{\Delta V_b(k-1)}\right)\Delta V_b(k) \tag{7}$$

where m' is positive suppression factor. The variable f(x) is a nonlinear function, which is defined as

$$f(x) = \exp(-x^2). \tag{8}$$

The output of the function is limited within the interval [0, 1]. The total stimulation received by the B cells is based on immune-based feedback law, which is given by

$$B(k) = \mathrm{TH}(k) - \mathrm{TS}(k)$$
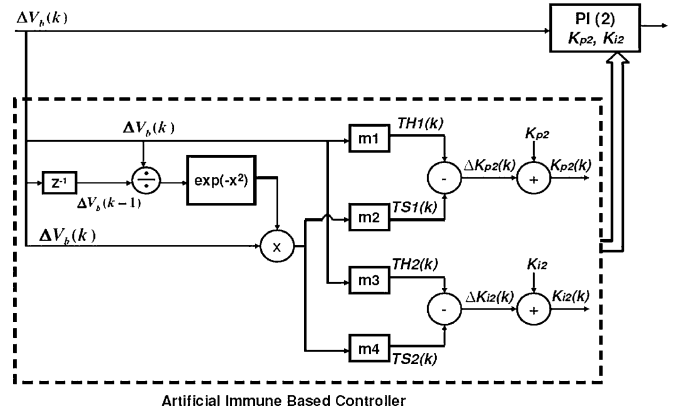$$B(k) = \left[m - m'f\left(\frac{\Delta V_b(k)}{\Delta V_b(k-1)}\right)\right]\Delta V_b(k). \tag{9}$$

So, the mechanism basically consists of two actions: once the antigens are found, the TH cells work to eliminate them, whereas the TS cells work to inhibit the actions of other cells. Fig. 5 illustrates this action of immune-based adaptive controller for the disturbance $\Delta V_b(k)$, where the parameters for the second PI controller [PI(2)] are modified online based on AIS. A similar figure can be drawn for the disturbance $\Delta V_{\rm CAP}(k)$, which dynamically modifies the parameters associated with the first PI controller [PI(1)].

In this paper, for the real-time implementation, the AIS-based control strategy is implemented on a DSP. Each AIS-based PI controller is associated with four "m" constants, as shown in Fig. 5. So, there are, as a whole, eight "m" constants (m_1–m_8), stimulation and suppression, for two PI controllers that are first tuned using PSO. The optimal values of these eight "m" constants are determined using the PSO algorithm. The dimensions of each particle of PSO are eight in this case, and are initially set to random values by the DSP at the start. Here, the signals $\Delta V_b(k)$ and $\Delta V_{\rm CAP}(k)$ are sent to the DSP from RTDS in order to take the helping and suppressing actions. Also, $\Delta V_b(k)$ is used for the calculation of cost function, as mentioned before. The control signal $B(k)$, which is basically the adaptive deviation in the values of proportional and integral gains of the PI controllers, are generated by the AIS-based controller implemented on the DSP. These signals are scaled and brought within the range -10 to $+10$ V, and sent back to RTDS. Inside the RTDS, these signals are again restored to their original values and added to the optimal values of the PI controller parameters to make them adaptive.

The optimal stimulation ($m_1, m_3, m_5,$ and m_7) and suppression ($m_2, m_4, m_6,$ and m_8) constants determined by PSO for MATLAB-based system are $m_1 = 189.06$, $m_2 = 118.21$, $m_3 = 122.61$, $m_4 = 416.7$, $m_5 = 5.01$, $m_6 = 1.33$, $m_7 = 450.37$, and $m_8 = 220.11$.

The optimal stimulation ($m_1, m_3, m_5,$ and m_7) and suppression ($m_2, m_4, m_6,$ and m_8) constants determined by PSO for RTDS-based system are $m_1 = 110.0$, $m_2 = 55.672$, $m_3 = 194.00$, $m_4 = 280.2$, $m_5 = 366.71$, $m_6 = 316.24$, $m_7 = 230.01$, and $m_8 = 43.0$.
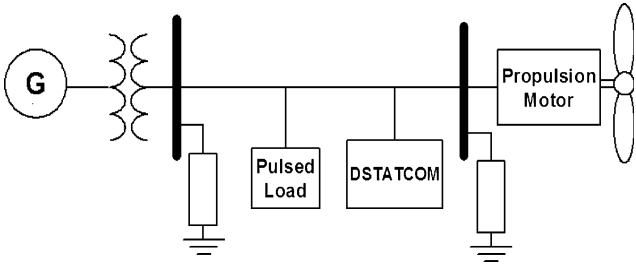
Fig. 6.   Test shipboard power system for MATLAB implementation.

V. TEST SYSTEM

As discussed earlier, the AIS-based adaptive control strategy is evaluated with two test systems: 1) MATLAB-based test system and 2) RTDS-based test system.

A. MATLAB-Based Test System

The ship power system actually consists of four generators and two propulsion motors. But, due to its symmetry, the effect of DSTATCOM and the adaptive control action can be studied easily with a simplified system having only one generator and one propulsion motor. For this paper, a simulation model having a generator of 36 MW/45 MVA and a propulsion motor of 10 MW is built in Simulink using the SimPowerSystem blocks. The single-line diagram of this system is shown in Fig. 6. A pulse load of 20 MW/20 MVAR having 200 ms duration is used for tuning the controller parameters using PSO. Whereas, the performance of the immune-based adaptive controller is observed for pulse loads of 20 MW/40 MVAR having duration of 100 and 200 ms, and 20 MW/50 MVAR for 200 ms.

B. RTDS-Based Test System

A relatively detail model of a ship power system having one main generator of 45 MVA, one auxiliary generator of 5 MVA, and one propulsion motor of 36 MW with voltage-source converter drives is designed with the help of RSCAD software of RTDS. Fig. 20 in the Appendix shows the RSCAD model of the test system used in this paper. Small time-step model ($1.5 \ \mu s$) of the propulsion motor, and the VSC are built up and interfaced with the remaining large time-step portion of the model through two interfacing transformers (see Fig. 21 in the Appendix). The optimal PI controller parameters and the "m" constants are determined using PSO for a pulse load of 20 MW/20 MVAR with a duration of 200 ms.

VI. RESULTS

A. MATLAB-Based Test System

As the DSTATCOM controller is tuned by PSO for a specific operating range, it achieves an innate immunity toward the pulse load disturbances close to this range. So, the AIS-based adaptive controller action cannot be distinguished for a pulse load of the same range. To observe the effect of AIS control strategy, two unusual disturbances are simulated. The first one is a pulse load of 20 MW/40 MVAR with duration of 200 ms, and the second one is the worst operating condition with a pulse load of 20 MW/50 MVAR and duration 200 ms.
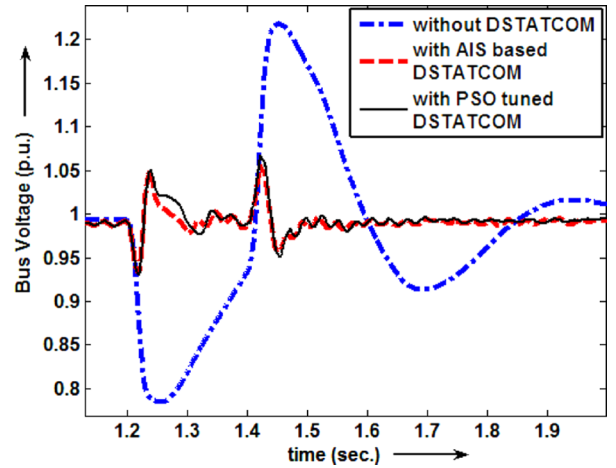

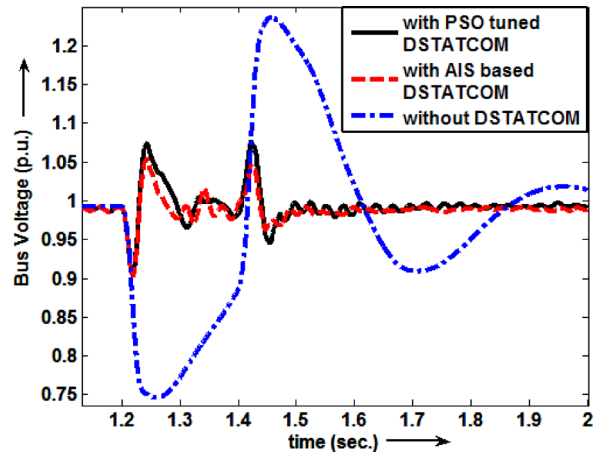Fig. 7.   Performance comparison for pulse load of 20 MW/40 MVAR for 200 ms.

Fig. 8.   Performance comparison for pulse load of 20 MW/50 MVAR for 200 ms.

The performance of the PSO-tuned DSTATCOM controller and the AIS-based adaptive controller are compared with each other as well as with a system having no DSTATCOM connected to it. Figs. 7 and 8 represent these cases.

It is found that both PSO-tuned controller and the AIS-based adaptive controller have a better performance than the system without a DSTATCOM. Also, Fig. 9, which is basically the zoomed version of Fig. 7, shows the improvement due to the AIS-based control with respect to the PSO-tuned controller. It is found that the peak value of the bus voltage is reduced by a small amount, and the postdisturbance voltage ripples damp out earlier.

If the operating condition is changed further to increase the magnitude of the pulse load to 20 MW/50 MVAR, the performance of the AIS-based controller is much better than the PSO-tuned controller. This is shown by Fig. 10, which is again a zoomed version of Fig. 8. Here, both the peak overshoot and the settling time are reduced by a noticeable amount. So, it is evident from the figures that the performance of the AIS-based adaptive control strategy gradually becomes significant with the increased severity of the system disturbance. This is the benefit of this adaptive control strategy.
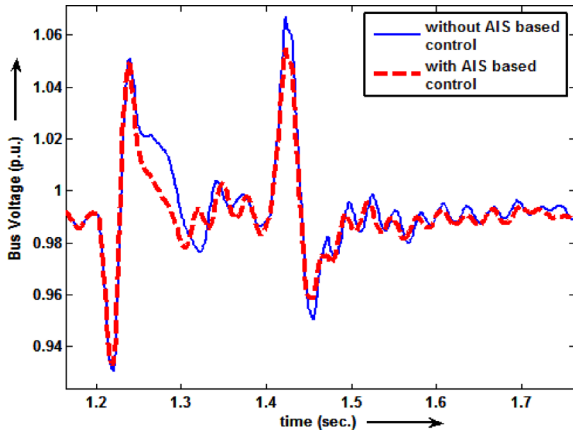
Fig. 9.   Performance comparison between PSO- (without AIS) and AIS-based controller for 20 MW/40 MVAR pulse load.
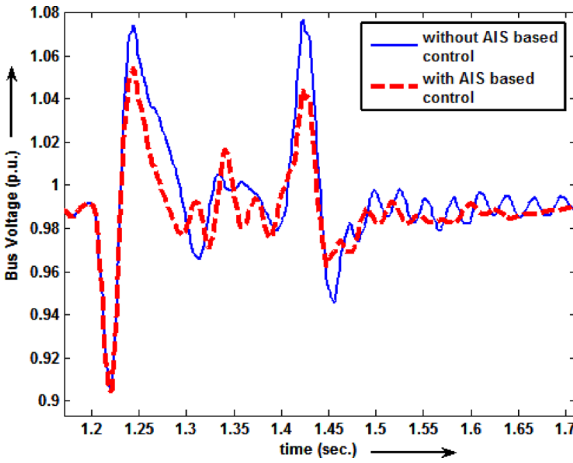

Fig. 10.   Performance comparison between PSO- (without AIS) and AIS-based controller for 20 MW/50 MVAR pulse load.

Fig. 11.   Variation of controller parameters Kpv and Kiv.

Fig. 12.   Variation of controller parameters Kpc and Kic.

Fig. 13.   Schematic representation of the pulse load and charging circuit.

Finally, Figs. 11 and 12 show the variation of the controller parameters during a disturbance at the third operating point.

The variation in the controllers' parameters indicates how the AIS-based adaptive control action is taken, and how the parameters adjust themselves with the continuously changing environment. Once the system returns to normality, the innate controller parameters are restored. This is the beauty of such a controller strategy.

B. RTDS-Based Test System

Based on the effective performance of the adaptive control strategy in the MATLAB environment, it is then implemented in a real-time environment. The real-time study has the following two sections.

1) Realistic Pulse Load Representation: In a practical ship power system, pulse loads are measured in kilojoules, megajoules, or even in gigajoules depending on the energy demand of the weapon systems. Due to the high-energy demand of pulse loads, they are generally associated with an additional energy storage device like flywheel and a charging circuit [1]. The energy storage device is not the focus of this paper, and hence, is
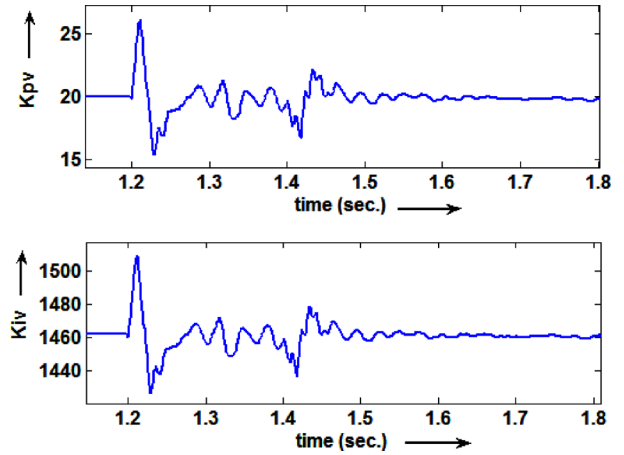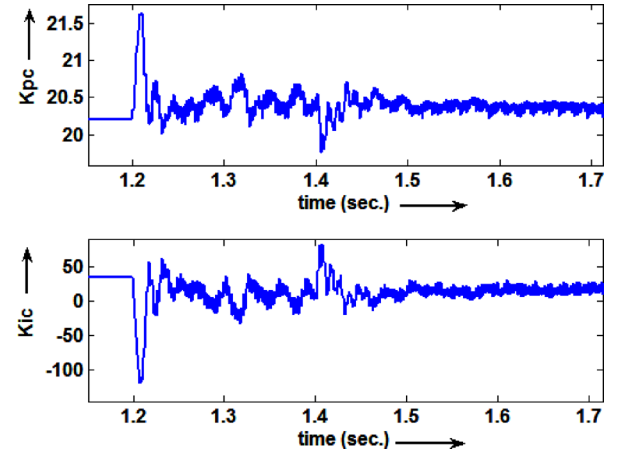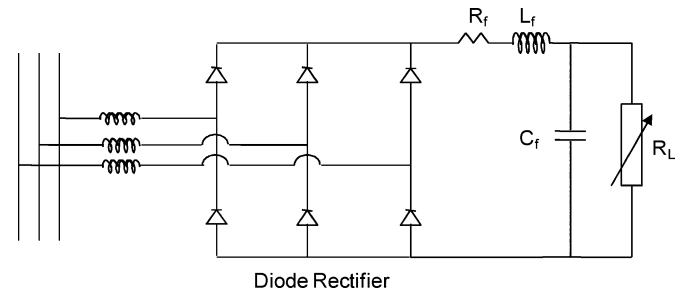
not considered here. But, a realistic representation of pulse load and its charging circuit is simulated in this paper. The charging circuit is represented by a variable resistance connected to the system via a diode rectifier and a charging capacitor (see Fig. 13). Initially, the resistance is kept very high so that it is almost open-circuited. Triggering of the pulse load means decreasing the value of the variable resistance suddenly, so that the capacitor discharges through it instantaneously and a charging current also flows from the system to the capacitor. Due to this sudden discharging and charging, a severe voltage dip and subsequent oscillation is noticed at the ac bus.
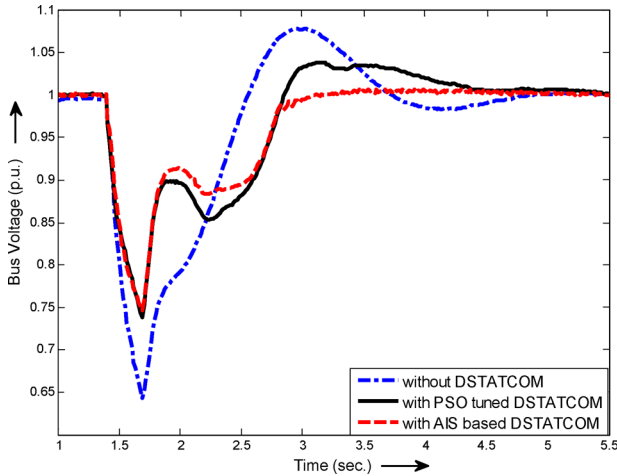
Fig. 14. Comparison of bus voltage characteristics for a 3.6 MJ realistic pulse load representation.

Fig. 15. Comparison of bus voltage characteristics for a 6-MJ realistic pulse load representation.

The performance of the AIS-based control strategy is now studied with different values of realistic pulse load disturbances. When the values are smaller than 3 MJ, it is found that there is hardly any difference between the performance of the PSO-tuned and AIS-based controller. But, as the magnitude of the pulse load is increased, better performance is observed with the AIS-based control. The performances of PSO-tuned and AIS-based controllers for a pulse load of 3.6 MJ is depicted in Fig. 14.

From Fig. 14, it can be seen that both PSO-tuned and AIS-based controls could reduce the voltage dip to some extent compared to the system without DSTATCOM. It is also observed that the postdisturbance overshoot is negligible with the AIS-based control strategy compared to that with the PSO-tuned controller. Another pulse load of magnitude 6 MJ is now simulated, and the performances of the controllers are depicted in Fig. 15. Again, it is observed that the AIS-based control is capable of reducing the postdisturbance oscillation faster than the PSO-tuned controller, and the bus voltage is settling down to the steady-state value much earlier with the AIS-based controller. The PSO-tuned controller produced an overshoot, which is almost equal to the system without a DSTATCOM, which means that the optimal values of the controller parameter are no longer "optimal" for this unusual disturbance. The system's innate immunity is not sufficient to handle wide ranges of pulse loads. So, the system needs adaptive immunity, which is provided by the AIS-based control strategy. The dynamic variations of controller parameters for 6 MJ pulse load are shown in Fig. 16. It is clearly observed that the parameters vary from their optimal values during disturbance due to the dominance of the stimulating action, and when the system comes back to its original steady state condition, the parameters again settle down to their optimal values due to the suppressing action of the immune feedback mechanism.

As mentioned earlier, with additional energy storage devices, the pulse load can vary up to the level of gigajoules in practical battle conditions. But, since no energy storage device is used in this study and the DSTATCOM has limitations in supplying active power, it is observed for this test system that the voltage dip cannot be improved further with the application of DSTAT-
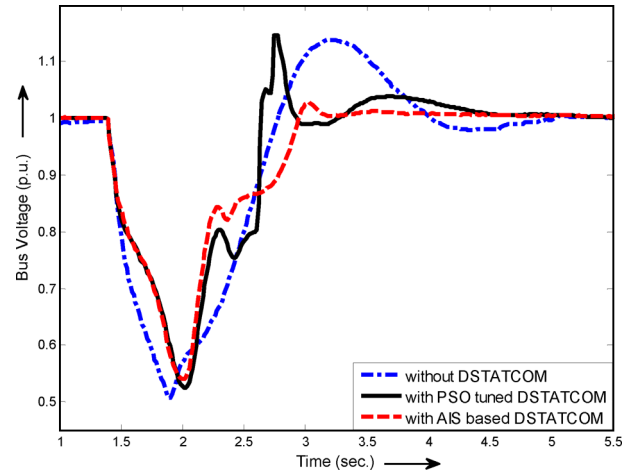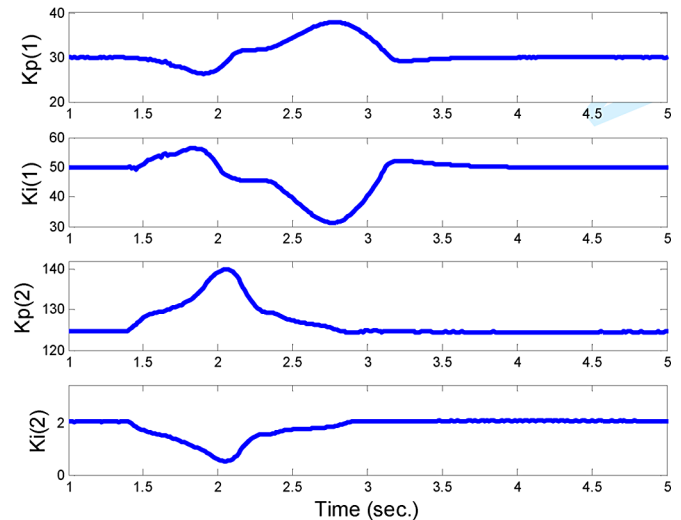

Fig. 16. Dynamic variation of parameters of PI controllers for 6 MJ pulse load.

COM if a realistic pulse load of 6 MJ or above is applied. But, the DSTATCOM can damp out the postpulse load oscillations quickly by controlling the reactive power injection. The role of DSTATCOM in controlling the voltage dip as well as the postdisturbance oscillation can also be prominently observed if the load contains certain amount of reactive power. Hence, some futuristic scenarios of pulse loads containing a large amount of reactive power are also studied to observe the performance of the AIS-based control strategy in worst hypothetical cases.

2) Futuristic Worst-Case Scenarios: The performance of the controller is first studied with a moderate disturbance that is close to the disturbance at which the controller is tuned using PSO (innate performance). Fig. 17 compares the performance of a PSO-tuned controller, an AIS-based adaptive controller, and a system without a DSTATCOM for the pulse loads of magnitude 20 MW/30 MVAR and having durations of 200 ms. It is again observed that both PSO-tuned controller and the AIS-based controller are able to stabilize the PCC bus voltage after the withdrawal of the pulse load without any significant
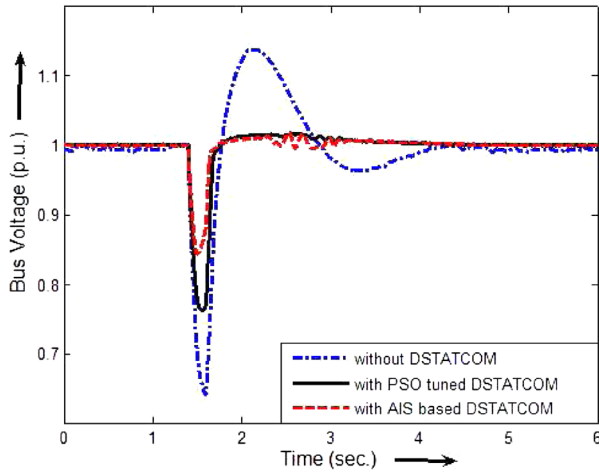
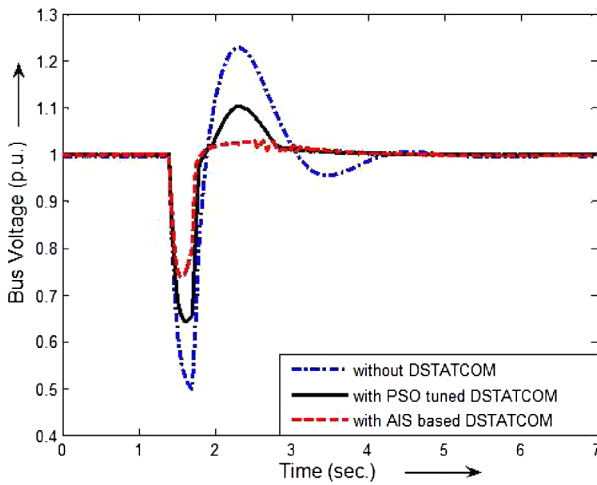Fig. 17. Performance comparison for pulse load of 20 MW/30 MVAR for 200 ms.

Fig. 18. Performance comparison for pulse load of 20 MW/40 MVAR for 300 ms.

Fig. 19. Dynamic variation of the PI controller parameters for 20 MW/40 MVAR pulse load.

overshoot. Whereas, the system without DSTATCOM has a large overshoot when the pulse load is withdrawn. Also, the voltage dip is minimized with PSO- and AIS-based controllers as compared to the system without DSTATCOM. For this moderate disturbance, the AIS-based controller is superior than the PSO-tuned controller only in terms of the voltage dip, which is least with the AIS-based controller.

Now, a severe pulse load disturbance of magnitude 20 MW/40 MVAR and duration 300 ms is applied to the test system. Fig. 18 compares the performances of PSO- and AIS-based controllers, and the system without DSTATCOM. It is observed that as the severity of the pulse load is increased, the action of AIS-based adaptive controller has become more significant. In Fig. 18, it is clearly observed that though the PSO-tuned controller produces an overshoot, the AIS-based controller does not. Also, the voltage dip is less with the AIS-based control strategy.

Finally, Fig. 19 shows the dynamic variation of the PI controller parameters for the 20 MW/40 MVAR pulse load disturbance. Once again, as the system returns to normality, the innate controller parameters are restored.
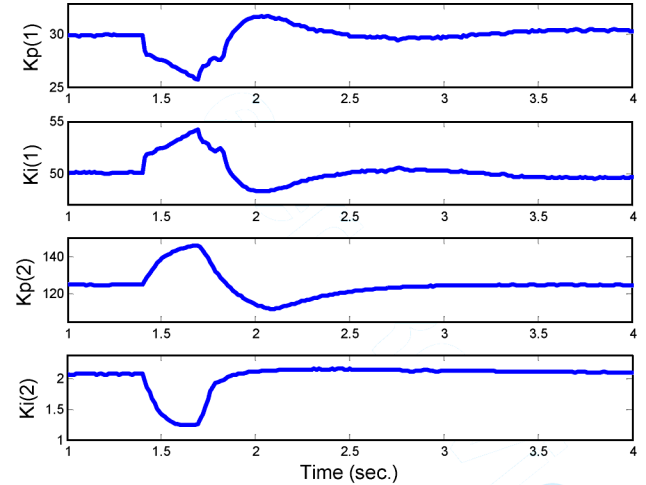
VII. CONCLUSION

An adaptive control strategy for a DSTATCOM based on AIS has been presented. Innate immunity to common disturbances is achieved using a controller whose optimal parameters are determined by PSO algorithm. For unknown, random, and severe disturbances, adaptive immunity is developed based on immune feedback principles. The performance of the proposed controller is validated through both MATLAB and real-time implementations. The results show that the voltage regulation at the PCC is much better with a properly tuned DSTATCOM. Also, it is evident from the two types of case studies, one representing the realistic pulse loads and the other representing some hypothetical worst-case scenarios, that as the system faces severe and unexpected disturbances, the role of AIS-based adaptive controller becomes more prominent. This ensures a better survivability of an electric ship against unusual system disturbances created by pulse loads.

The beauty of the proposed adaptive controller is that the original optimal controller parameters are restored as the system returns to normality. This is unique for a controller that is adaptive. Such an adaptive controller has the potential for effective control of power electronics devices operating in nonlinear environments.

Future study on implementing the AIS control strategy on a physical DSTATCOM hardware and validating the effectiveness of the controller on an electric ship power system remains to be investigated. The adaptive AIS control strategy presented in this paper has potential for applications in the smart power grid environment where there are possibilities of unforeseen energy and load fluctuations.

APPENDIX

Figs. 20 and 21 show the RSCAD model of the test system used in this paper and the small time-step model (1.5 μs) of the propulsion motor with VSC, respectively.
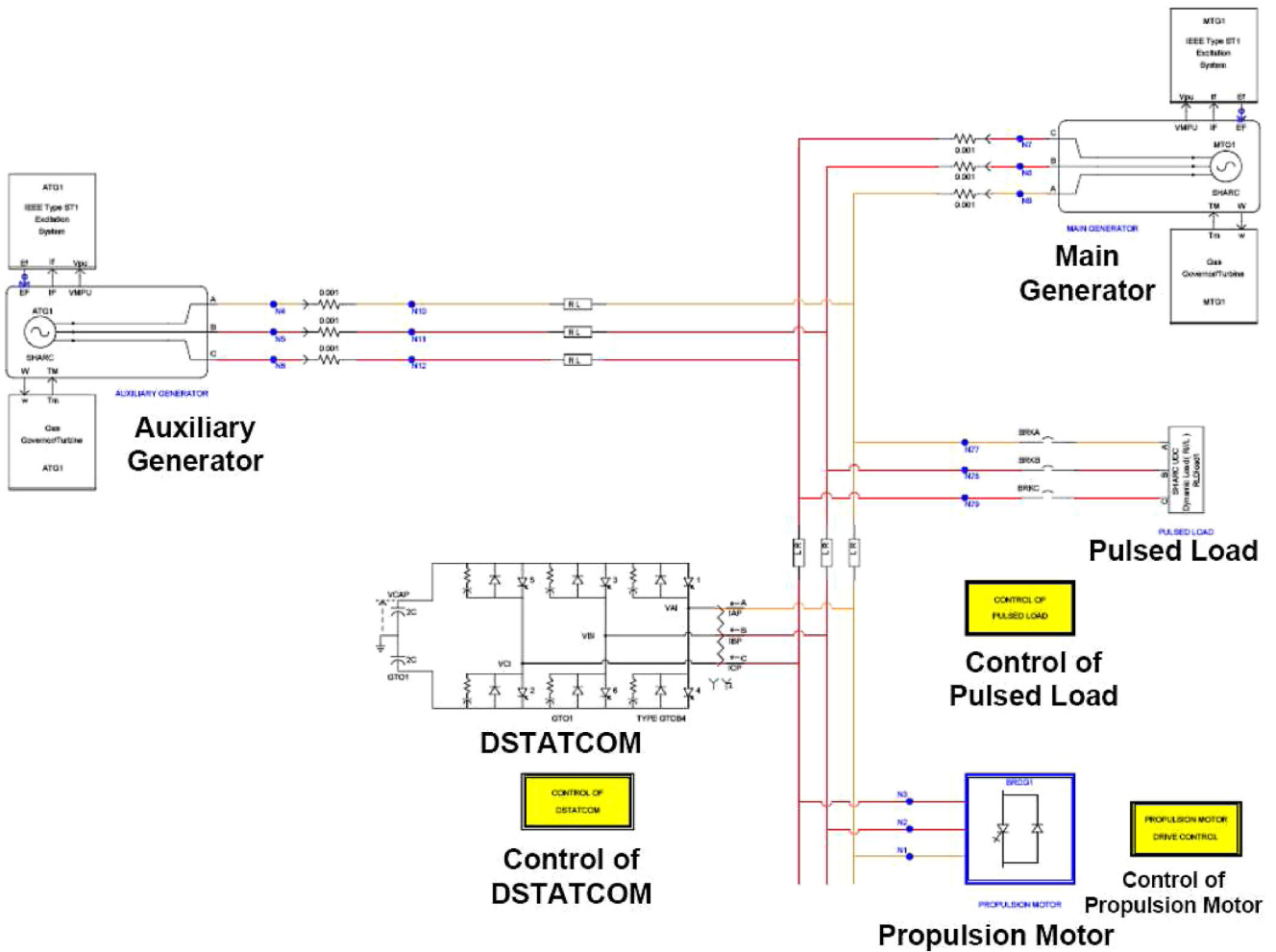
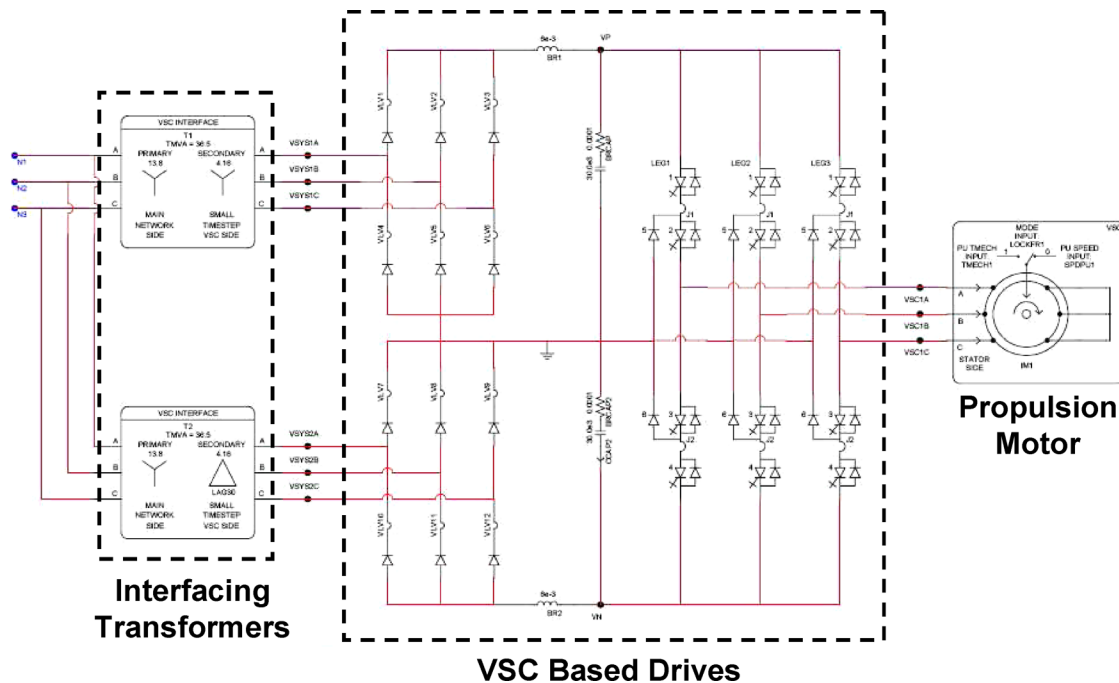Fig. 20.   RSCAD model of the test system.

Fig. 21.   Small time-step model of the propulsion motor with VSC.

REFERENCES

[1] M. Steurer, M. Andrus, J. Langston, L. Qi, S. Suryanarayanan, S. Woodruff, and P. F. Ribeiro, "Investigating the impact of pulsed power charging demands on shipboard power quality," in *Proc. IEEE Electr. Ship Technol. Symp. (ESTS 2007)*, pp. 315–321.

[2] T. A. Baginski and K. A. Thomas, "A robust one-shot switch for high-power pulse applications," *IEEE Trans. Power Electron.*, vol. 24, no. 1, pp. 253–259, Jan. 2009.

[3] A. Shukla, A. Ghosh, and A. Joshi, "Control schemes for DC capacitor voltages equalization in diode-clamped multilevel inverter-based DSTAT-COM," *IEEE Trans. Power Del.*, vol. 23, no. 2, pp. 1139–1149, Apr. 2008.

[4] A. Ghosh and G. Ledwich, "Application of power electronics to power distribution system," *IEEE Tutorial Course—IEEE Power Engineering Society, No. 05TP176, IEEE PES General Meeting*, San Francisco, USA, 2005.

[5] M. K. Mishra, A. Joshi, and A. Ghosh, "Control schemes for equalization of capacitor voltages in neutral clamped shunt compensator," *IEEE Trans. Power Del.*, vol. 18, no. 2, pp. 538–544, Apr. 2003.

[6] A. Shukla, A. Ghosh, and A. Joshi, "Hysteresis current control operation of flying capacitor multilevel inverter and its application in shunt compensation of distribution systems," *IEEE Trans. Power Del.*, vol. 22, no. 1, pp. 396–405, Jan. 2007.

[7] A. Shukla, A. Ghosh, and A. Joshi, "State feedback control of multilevel inverters for DSTATCOM applications," *IEEE Trans. Power Del.*, vol. 22, no. 4, pp. 2409–2418, Oct. 2007.

[8] R. Gupta and A. Ghosh, "Frequency-domain characterization of sliding mode control of an inverter used in DSTATCOM application," *IEEE Trans. Circuits Syst. I, Reg. Papers*, vol. 53, no. 3, pp. 662–676, Mar. 2006.

[9] M. A. Eldery, E. F. El-Saadany, and M. M. A. Salama, "Sliding mode controller for pulse width modulation based DSTATCOM," in *Proc. Can. Conf. Electr. Comput. Eng. (CCECE 2006)*, pp. 2216–2219.

[10] Y. Xiao-Ping, Z. Yan-Ru, and W. Yan, "A novel control method for DSTATCOM using artificial neural network," in *Proc. CES/IEEE 5th Int. Power Electron. Motion Control Conf. (IPEMC 2006)*, Aug. 14–16, vol. 3, pp. 1–4.

[11] B. Singh, J. Solanki, and V. Verma, "Neural network based control of reduced rating DSTATCOM," in *Proc. Annu. IEEE Conf. INDICON*, Dec. 11–13, 2005, pp. 516–520.

[12] M. Hunjan and G. K. Venayagamoorthy, "Adaptive power system stabilizers using artificial immune system," in *Proc. IEEE Symp. Artif. Life (CI-ALife 2007)*, pp. 440–447.

[13] D. Dasgupta and S. Forrest, "Artificial immune systems in industrial applications," in *Proc. 2nd Int. Conf. Intell. Process. Manuf. Mater.*, 1999, vol. 1, pp. 257–267.

[14] P. Mitra and G. K. Venayagamoorthy, "Artificial immune system based DSTATCOM control for an electric ship power system," in *Proc. 39th IEEE Power Electron. Spec. Conf. (PESC 2008)*, Jun. 15–19, pp. 718–723.

[15] S. Kannan, S. Jayaram, and M. M. A. Salama, "Real and reactive power coordination for a unified power flow controller," *IEEE Trans. Power Syst.*, vol. 19, no. 3, pp. 1454–1461, Aug. 2004.

[16] Y. del Valle, G. K. Venayagamoorthy, S. Mohagheghi, J. Hernandez, and R. G. Harley, "Particle swarm optimization: Basic concepts, variants and applications in power system," *IEEE Trans. Evol. Comput.*, vol. 12, no. 2, pp. 171–195, Apr. 2008.

Pinaki Mitra (S'08) was born in 1974. He received the B.E. degree in electrical engineering in 1997 and the M.E. degree in electrical machines in 1999 from Jadavpur University, Kolkata, India. He is currently working toward the Ph.D. degree at the Real-Time Power and Intelligent Systems Laboratory, Department of Electrical and Computer Engineering, Missouri University of Science and Technology, Rolla.

His current research interest include the application of computational intelligence techniques in the area of control and reconfiguration of electric ship power systems and smart grids.

Ganesh Kumar Venayagamoorthy (S'91–M'97–SM'02) received the B.Eng. degree (with first class honors) in electrical and electronics engineering from Abubakar Tafawa Balewa University, Bauchi, Nigeria, in 1994, and the M.Sc.Eng. and Ph.D. degrees in electrical engineering from the University of Natal, Durban, South Africa, in 1999 and 2002, respectively.

He was a Senior Lecturer at Durban University of Technology, South Africa. In May 2002, he joined Missouri University of Science and Technology (Missouri S & T), Rolla, where he is currently an Associate Professor of electrical and computer engineering and the Director of the Real-Time Power and Intelligent Systems Laboratory. During summer of 2007, he was a Visiting Researcher at ABB Corporate Research Center, Sweden. He has authored or coauthored two edited books, five book chapters, 70 refereed journals papers, and over 250 refereed international conference proceeding papers. His current research interests include the development and applications of computational intelligence methods for solving real world problems including smart grids, power systems stability and control, power electronics, alternative sources of energy, sensor networks, signal processing, and evolvable hardware.

Dr. Venayagamoorthy was an Associate Editor of the IEEE TRANSACTIONS ON NEURAL NETWORKS from 2004 to 2007, and the IEEE TRANSACTIONS ON INSTRUMENTATION AND MEASUREMENT in 2007. He is a Senior Member of the International Neural Network Society and a member of the Board of Governors. He is a Fellow of the Institution of Engineering and Technology, U.K., and the South Institute of Electrical Engineers. He was a recipient of the 2008 IEEE St. Louis Section Outstanding Educator Award, the 2007 Office of Naval Research (ONR) Young Investigator Program Award, the 2004 National Science Foundation (NSF) CAREER Award, the 2006 IEEE Power Engineering Society Walter Fee Outstanding Young Engineer Award, the 2006 IEEE St. Louis Section Outstanding Section Member Award, the 2005 IEEE Industry Applications Society (IAS) Outstanding Young Member Award, the 2005 South African Institute Of Electrical Engineers (SAIEE) Young Achievers Award, the 2004 IEEE St. Louis Section Outstanding Young Engineer Award, the 2003 International Neural Network Society (INNS) Young Investigator Award, the 2001 IEEE Computational Intelligence Society (CIS) Walter Karplus Summer Research Award, seven prize papers from the IEEE IAS and IEEE CIS, a 2007 Missouri S & T Teaching Commendation Award, a 2006 Missouri S & T School of Engineering Teaching Excellence Award, and a 2008, 2007, and 2005 Missouri S & T Faculty Excellence Award.